

Coordination and Dehydrogenation of Diphosphine-Borane $\text{Ph}_2\text{PCH}_2\text{PPh}_2\cdot\text{BH}_3$ at a Heterometallic MoRe Center to Give an Agostic Boryl-Bridged Derivative

M. Angeles Alvarez, M. Esther García, Daniel García-Vivó,* Estefanía Huergo, and
Miguel A. Ruiz.*

*Departamento de Química Orgánica e Inorgánica/IUQOEM, Universidad de Oviedo,
E-33071 Oviedo, Spain.*

Abstract

The coordination chemistry of the title diphosphine-borane adduct at heterometallic MoRe centers was examined through its reactions with the hydride complex $[\text{MoReCp}(\mu\text{-H})(\mu\text{-PCy}_2)(\text{CO})_5(\text{NCMe})]$ ($\text{Cp} = \eta^5\text{-C}_5\text{H}_5$). The latter reacted rapidly with stoichiometric amounts of $\text{dppm}\cdot\text{BH}_3$ ($\text{dppm} = \text{Ph}_2\text{PCH}_2\text{PPh}_2$) in refluxing toluene solution, with displacement of the nitrile ligand, to give $[\text{MoReCp}(\mu\text{-H})(\mu\text{-PCy}_2)(\text{CO})_5(\kappa^1_{\text{P}}\text{-dppm}\cdot\text{BH}_3)]$, with a *P*-bound diphosphine-borane ligand arranged *trans* to the PCy_2 group. Decarbonylation of the latter complex was accomplished rapidly upon irradiation with visible-UV light in toluene solution at 263 K, to give the agostic derivative $[\text{MoReCp}(\mu\text{-H})(\mu\text{-PCy}_2)(\text{CO})_4(\kappa^1_{\text{P}}, \eta^2\text{-dppm}\cdot\text{BH}_3)]$ as major product ($\text{Mo-Re} = 3.2075(5) \text{ \AA}$), along with small amounts of the diphosphine-bridged complex $[\text{MoReCp}(\mu\text{-H})(\mu\text{-PCy}_2)(\text{CO})_4(\mu\text{-dppm})]$. Extended photolysis of the agostic complex at 288 K promoted an unprecedented dehydrogenation process involving the borane group and the hydride ligand, to give the diphosphine-boryl complex $[\text{MoReCp}(\mu\text{-}\eta^2:\kappa^2_{\text{P,B}}\text{-H}_2\text{B}\cdot\text{dppm})(\mu\text{-PCy}_2)(\text{CO})_4]$ ($\text{Mo-Re} = 3.075(1) \text{ \AA}$). The latter displayed a boryl ligand in a novel bridging coordination mode, it being σ -bound to one of the metal atoms ($\text{B-Re} = 2.38(2) \text{ \AA}$) while interacting with the second metal atom *via* a strong *side-on* tricentric B-H-M interaction ($\text{B-Mo} = 2.31(1)$; $\text{H-Mo} = 1.9(1) \text{ \AA}$). The overall dehydrogenation process was endergonic by 43 kJ/mol, according to Density Functional Theory calculations.

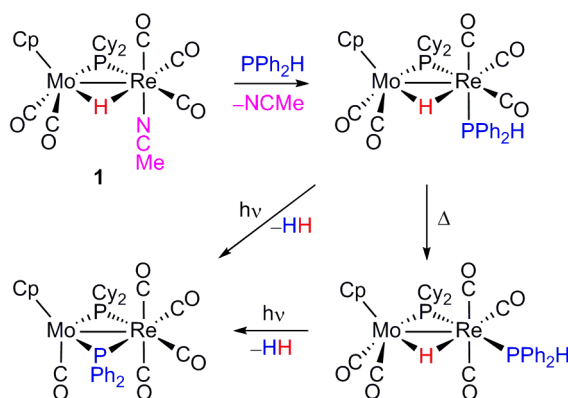
Introduction

Transition-metal complexes holding two distinct metal atoms in close proximity (heterometallic complexes) display singular reactivity patterns derived from the different electronic and coordination environment of their metal centers, which produces cooperative and synergic effects eventually leading to reactivity not observed

for related homometallic complexes, as concerning both stoichiometric and catalytic processes.¹ Binuclear heterometallic complexes displaying metal-metal multiple bonds are a particularly interesting group within this large family of species, as the intermetallic multiple bond additionally provides electronic and coordinative unsaturation to the dimetal center, which further enhances its reactivity.² Research in this area, however, has been relatively ill-developed for organometallic complexes, due to scarcity in the number of available substrates suitable for extensive reactivity studies.³

Recently, we implemented an efficient synthetic procedure for the hydride complex [MoReCp(μ -H)(μ -PCy₂)(CO)₅(NCMe)] (**1**) which, while being itself an electron-precise species, undergoes displacement of the nitrile ligand by different molecules under mild conditions, whereby it effectively acts as a surrogate of the unsaturated hydride [MoReCp(μ -H)(μ -PCy₂)(CO)₅] (Cp = η^5 -C₅H₅).⁴ The latter is a very unstable molecule which cannot be even detected during protonation of the unsaturated anion [MoReCp(μ -PCy₂)(CO)₅]⁻ (Mo=Re),⁵ and the same applies to the analogous MoMn hydride complex.⁶

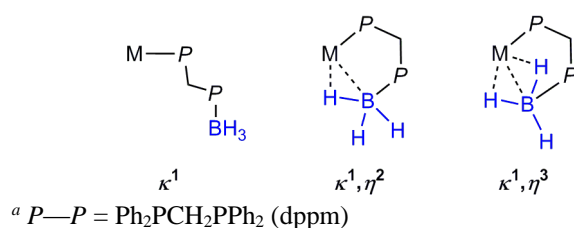
Scheme 1. PPh₂H Derivatives of Complex 1



Interestingly, compound **1** readily adds different molecules having E–H bonds (E = p-block element) such as secondary phosphines and thiols, a process which can be followed by the cleavage of the corresponding E–H bond under mild thermal or photochemical activation. For instance, PPh₂H readily displaces the MeCN ligand in **1** to give the corresponding phosphine derivative with retention of the stereochemistry, which then undergoes photochemical dehydrogenation to render a diphenylphosphido-bridged derivative, in a process involving both P–H bond cleavage and carbonyl rearrangement around the heterometallic center (Scheme 1).⁴ Dehydrogenation in this case cannot be promoted thermally, which instead just induces a rearrangement of the phosphine ligand, to a position *trans* to the PCy₂ group, more favored on steric grounds.^{5b}

We then turned our attention to the potential use of compound **1** in the activation of B–H bonds. Since **1** failed to react with a simple borane adduct such as $\text{NH}_3 \cdot \text{BH}_3$, we decided to examine reactions with the diphosphine adduct $\text{dppm} \cdot \text{BH}_3$ ($\text{dppm} = \text{Ph}_2\text{PCH}_2\text{PPh}_2$), which is the purpose of the present work. It could be anticipated that the “free” phosphorus atom in the borane adduct would easily displace the acetonitrile ligand of **1**, then providing an opportunity for subsequent coordination of the B–H bonds at the heterometallic center. Indeed, previous work has shown that the $\text{dppm} \cdot \text{BH}_3$ ligand can form different mononuclear complexes by using the lone electron pair of its “free” P atom (the trivial κ^1 -mode), and additionally one or two B–H bonds (κ^1, η^2 - and κ^1, η^3 -modes, Chart 1).⁷⁻⁹ Incidentally, we note that only one binuclear complex with this ligand appears to have been reported previously (a Fe_2 complex with a conventional κ^1 -bound ligand).¹⁰ In addition, we note that the relatively weak interaction of B–H bonds with metal atoms in the agostic κ^1, η^2 - and κ^1, η^3 -modes enables $\text{dppm} \cdot \text{BH}_3$ to act as a hemilabile ligand, able to provide, by de-coordination of B–H bonds, vacant coordination sites useful in catalytic processes.¹¹ Finally, we should also mention that phosphine boranes and their metal complexes have been extensively studied as precursors for new main group materials.¹²

Chart 1. Known Coordination Modes of $\text{dppm} \cdot \text{BH}_3$ ^a



In this paper we report our results on the reactions of **1** with $\text{BH}_3 \cdot \text{dppm}$, and further decarbonylation studies aimed at involving the B–H bonds of this ligand in coordination to the heterometallic center. As will be shown below, this ligand first binds the dimetal center in a κ^1 -mode at the Re atom as expected, but then is able to adopt an agostic κ^1, η^2 -mode, and eventually undergoes an unprecedented dehydrogenation to render a very rare $\text{BH}_2 \cdot \text{dppm}$ derivative displaying a novel bridging coordination mode of the boryl ligand, which involves both two-center (B–Re) and three-center (B–H–Mo) interactions with the dimetal site.

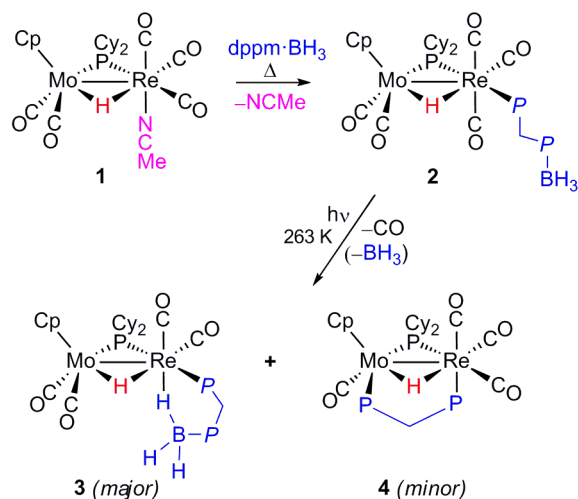
Results and Discussion

Diphosphine-Borane Derivatives of Complex 1. Adduct $\text{dppm} \cdot \text{BH}_3$ does not react with compound **1** in toluene solution at room temperature, but does it rapidly under reflux conditions (ca. 383 K), to give the diphosphine-borane derivative $[\text{MoReCp}(\mu\text{-H})(\mu\text{-PCy}_2)(\text{CO})_5(\kappa^1\text{P-dppm} \cdot \text{BH}_3)]$ (**2**) within a few minutes (Scheme 2). Compound **2**

bears a $\text{dppm}\cdot\text{BH}_3$ ligand P -bound at the Re atom and positioned *trans* to the PCy_2 group, as shown by spectroscopic data discussed below. It might be anticipated that formation of **2** should be initiated with displacement of MeCN to give an intermediate species bearing the diphosphine-borane ligand at the same coordination position as the leaving ligand, that is, *cis* to the bridging ligands, as observed in the reaction of **1** with PPh_2H (Scheme 1). This intermediate then would rearrange to a position *trans* to the PCy_2 group, thus minimizing the steric repulsions between these two relatively bulky P -donors; such rearrangement also involves a change in the disposition of carbonyls at the Re atom, from facial to a meridional one. In agreement with this, when reacting **1** and $\text{dppm}\cdot\text{BH}_3$ at lower temperature (333 K) we could detect the formation of such an intermediate species,¹³ with spectroscopic properties alike to those of *fac*- $[\text{MoReCp}(\mu\text{-H})(\mu\text{-PCy}_2)(\text{CO})_5(\text{PPh}_2\text{H})]$ (Scheme 1), although no attempts to isolate it were made.

Compound **2** is a thermally-robust molecule which remains unchanged in refluxing toluene solution for one hour. In contrast, it undergoes fast decarbonylation upon irradiation with visible-UV light at low temperature (263 K), to give the agostic complex $[\text{MoReCp}(\mu\text{-H})(\mu\text{-PCy}_2)(\text{CO})_4(\kappa^1\text{P}, \eta^2\text{-dppm}\cdot\text{BH}_3)]$ (**3**) as major product, along with small amounts of the diphosphine-bridged complex $[\text{MoReCp}(\mu\text{-H})(\mu\text{-PCy}_2)(\text{CO})_4(\mu\text{-dppm})]$ (**4**), from which it can be separated upon chromatographic workup (yields of isolated products 67 and 20%, respectively; see the Experimental section). The choice of experimental conditions in this photochemical reaction is critical to obtain **3**, as this agostic complex itself undergoes dehydrogenation upon extended photolysis at room temperature, a matter to be discussed later on.

Scheme 2. Diphosphine-Borane Derivatives of **1**^a



^a $P-P = \text{Ph}_2\text{PCH}_2\text{PPh}_2$ (dppm)

Although photochemically induced, the formation of **3** proceeds as it would have been expected for a thermal reaction, so that one of the carbonyls arranged *trans* to each other (thus experiencing the largest *trans* influence) is preferentially lost, with the

vacant coordination position thus generated being blocked by coordination of one of the B–H bonds of the dangling BH₃ group of **2**. The overall conformation of the resulting molecule, with the BH₃ group positioned *anti* with respect to the cyclopentadienyl ligand, is likely the most favored one on steric grounds. On the other hand, the formation of **4** can be understood as following from a side decomposition process whereby borane would be lost, along with CO.¹⁴ This could first yield a complex of type [MoReCp(μ -H)(μ -PCy₂)(CO)₄(κ^2 -dppm)] with a chelating dppm ligand at the Re atom, which then would rearrange into the bridging coordination mode, with one carbonyl ligand migrating from Mo to Re, to balance the coordination environments of the metal centers. In support of this hypothesis we note that previous work has revealed that the related chelate MoMn complex [MoMnCp(μ -H)(μ -PPh₂)(CO)₄(κ^2 -dppm)] rearranges into its dppm-bridged isomer [MoMnCp(μ -H)(μ -PPh₂)(CO)₄(μ -dppm)] upon irradiation with UV light.¹⁵ We note, however, that alternative reaction sequences might also explain the formation of the side-product **4**.

Structural Characterization of the Pentacarbonyl Complex 2. Spectroscopic data for **2** (Table 1, Experimental section, and SI) allows for a complete structural characterization of this molecule. Its IR spectrum displays five C–O stretches, with the two less energetic ones being likely associated with the cisoid Mo(CO)₂ fragment, while the weak intensity of the most energetic one (at 2031 cm⁻¹) denotes the presence of a T-shaped M(CO)₃ oscillator (meridional arrangement in octahedral geometries).¹⁶ The bridging hydride ligand in **2** gives rise to a NMR resonance at –13.09 ppm, a position similar to that in parent **1** (–11.12 ppm). This resonance now displays comparable couplings of 18 and 14 Hz to P atoms, indicating a cisoid positioning of the hydride relative to both Re-bound P atoms.¹⁷ In agreement with this, the PCy₂ group (δ_P 142.6 ppm) displays a large coupling of 70 Hz to the Re-bound atom of the diphosphine-borane ligand (–2.7 ppm), indicative of a transoid disposition of these two atoms (cf. 65 Hz in *mer*-[MoReCp(μ -H)(μ -PCy₂)(CO)₅(PPh₂H)].^{5b} In addition, the diphosphine fragment also gives rise to a broad resonance at 13.3 ppm denoting the bonding of the second P atom to a borane group, itself revealed by the presence of a broad resonance at –37.7 in the ¹¹B spectrum. We note that the latter data are comparable to those for the free dppm·BH₃ ligand (δ_{P-B} 16.9 ppm; δ_B –37.1 ppm),^{8b} as expected. The ¹H NMR resonance of the borane group in **2**, anticipated to be very broad, could not be clearly observed in the spectrum (Figure S3), as it was partially obscured by the resonances of the Cy hydrogens (cf. δ_H 0.99 ppm for the free ligand).

Table 1. Selected IR,^a and ³¹P{¹H} Data^b for New Compounds.^c

Compound	$\nu(\text{CO})$	$\delta(\text{PCy}_2)$	$\delta(\text{PBH}_n)$	$\delta(\text{PPh}_2)$
[MoReCp(μ -H)(μ -PCy ₂)(CO) ₅ (NCMe)] (1) ^d	2010 (s), 1938 (vs), 1917 (s), 1900 (s), 1859 (m)	139.0		
[MoReCp(μ -H)(μ -PCy ₂)(CO) ₅ (κ^1 -P-dppm·BH ₃)] (2)	2031 (w), 1939 (vs), 1925 (m, sh), 1912 (m, sh); 1855 (m)	142.6	13.3	-2.7
[MoReCp(μ -H)(μ -PCy ₂)(CO) ₄ (κ^1 -P, η^2 -dppm·BH ₃)] (3)	1932 (m, sh), 1913 (vs), 1844 (s)	153.1	15.5	17.9
[MoReCp(μ -H)(μ -PCy ₂)(CO) ₄ (μ -dppm)] (4)	2001 (vs), 1912 (s), 1896 (s), 1793 (m)	122.1		76.3, -14.6
[MoReCp(μ - η^2 : κ^2 -P,B-H ₂ B-dppm)(μ -PCy ₂)(CO) ₄] (5)	2017 (w), 1927 (vs), 1905 (m), 1761 (m)	184.5	23.7	10.5

^a Recorded in dichloromethane solution, with C–O stretching bands [$\nu(\text{CO})$] in cm⁻¹. ^b Recorded in CD₂Cl₂ solution at 162.16 MHz and 293 K, with chemical shifts (δ) in ppm. ^c dppm = Ph₂PCH₂PPh₂. ^d Data taken from reference 4; IR data in tetrahydrofuran solution.

Structure of the Agostic Complex 3. The structure of **3** in the crystal (Figure 1 and Table 2) is made up of MoCp(CO)₂ and Re(CO)₂ fragments bridged by hydride and phosphanide ligands. This completes the usual four-legged piano stool coordination geometry around the Mo atom. Besides this, a roughly octahedral coordination around rhenium is completed by the diphosphine-borane ligand, with its formerly “free” P atom bound *trans* to the PCy₂ group (P1–Re–P2 = 172.68(5)^o), and a B–H bond of the borane unit coordinated in a position *cis* to the bridging ligands, and *anti* with respect to the Mo-bound cyclopentadienyl ligand. As a result, the overall molecule becomes an electron-precise complex (34 electrons), for which a single intermetallic bond has to be proposed according to the 18-electron formalism. This is in agreement with the intermetallic length of 3.2075(5) Å, very close to the values of ca. 3.19 Å measured in the related complexes [MoReCp(μ -H)(μ -PCy₂)(CO)₅(NH₃)]^{5a} and [MoReCp(μ -H)(μ -PPh₂)(CO)₆],¹⁸ and only moderately longer than the reference value of 3.05 Å for a Mo–Re single bond.¹⁹ The M–P1 distances in **3** differ by ca. 0.11 Å which, after allowing for the 0.03 Å shorter covalent radius of Re (vs. Mo), still suggests a stronger binding of the PCy₂ ligand to the Re atom, possibly to balance the poorer donor properties of the coordinated B–H bond, when compared to conventional donors such as phosphines or CO.

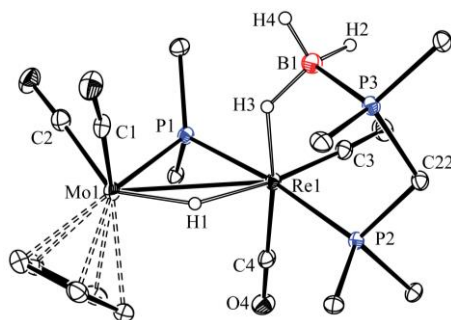


Figure 1. ORTEP diagram (30% probability) of compound **3** with Cy and Ph groups (except their C¹ atoms) and most H atoms omitted for clarity.

Table 2. Selected Bond Lengths (Å) and Angles (°) for Compound **3**

Mo1–Re1	3.2075(5)	Mo1–P1–Re1	82.56(4)
Mo1–P1	2.486(1)	P1–Mo1–C1	105.4(2)
Re1–P1	2.374(1)	P1–Mo1–C2	72.0(2)
Re1–P2	2.376(1)	P1–Mo1–H1	79(2)
Mo1–H1	1.80(7)	C1–Mo1–C2	80.1(2)
Re1–H1	1.95(7)	P1–Re1–P2	172.68(5)
Mo1–C1	1.940(6)	P1–Re1–C3	97.8(2)
Mo1–C2	1.960(6)	P1–Re1–C4	89.3(2)
Re1–C3	1.910(6)	P1–Re1–H1	79(2)
Re1–C4	1.890(6)	P1–Re1–H3	89(2)
Re1–B1	2.843(7)	P2–Re1–C3	89.0(2)
Re1–H3	1.88(7)	P2–Re1–C4	87.8(2)
B1–H3	1.23(7)	Re1–H3–B1	130(4)
B1–H2	1.11(7)	C3–Re1–C4	91.1(2)
B1–H4	1.10(7)		
P3–B1	1.922(6)		

As for the binding of the borane group to Re, we note that the coordinated B–H bond (1.23(7) Å) appears to be longer than the other two ones (ca. 1.10 Å) as expected, but the low precision of these data precludes any further analysis. We note, however, that a genuine enlargement of this bond is supported by DFT calculations to be discussed later on. The tricentric Re–H–B interaction renders a Re–H separation (1.88(7) Å) comparable to the one resulting from the Mo–H–Re interaction, a rather large Re–H–B angle of 130(4)°, and a very large Re···B separation of 2.843(7) Å, the latter being far above the reference figure of 2.35 Å for a Re–B single bond.¹⁹ These geometrical parameters suggest that the tricentric Re–H–B interaction in **3** should be better classified as one of the *end-on* type.²⁰ Indeed, a search on the Cambridge Crystallographic Database revealed that this coordination type typically involves Re···B separations in the range 2.70–2.85 Å and Re–H–B angles of 115–150°.²¹ Thus, we can properly speak of an extreme *end-on* coordination to Re of the B–H bond in compound **3**, it actually being only exceeded by that found in the mononuclear complex *fac*-[Re{ $\kappa^2_{s,s}, \eta^2$ -H₂B(timMe)(bzt)}(CO)₃] (Re···B = 2.862(5) Å, Re–H–B ca. 130°).²² This structural feature is possibly related to the presence in these complexes of a carbonyl ligand (with a strong *trans* influence) *trans* to the coordinated B–H bond. In line with this interpretation, we note that the chromium complex [Cr(CO)₄(κ^1, η^2 -dppm·BH₃)] also displays a very large Cr···B separation of 2.800(2) Å (Cr–H–B = 130(1)°),^{8b} and the same seems to hold for simple η^2 -complexes of phosphine-borane adducts (cf. W···B = 2.86(2) Å for [W(CO)₅(η^2 -PMe₃·BH₃)]).²³

Spectroscopic data for compound **3** (Table 1, Experimental section and SI) are consistent with the structure found in the solid state, and support its retention in solution. The IR spectrum of **3** displays three C–O stretches, with the most energetic one being of medium intensity, which is consistent with the presence of a [M(CO)₂]₂ oscillator made of cisoid M(CO)₂ fragments positioned close to an *anti* arrangement.¹⁶

The transoid positioning of P atoms around rhenium is indicated by the large P-P coupling of 100 Hz between PCy₂ and PPh₂ groups, but we note that the latter P atom now is more deshielded than in the precursor **2** (δ_{P} 17.9 vs. -2.7 ppm). This might be attributed to the formation of the chelate ring (a five-membered one, if taking into account the weak Re...B interaction) when going from **2** to **3**, an effect well known for chelating diphosphine and related bidentate ligands.²⁴ In contrast, the Ph₂PBH₃ fragment gives rise to ³¹P (δ_{P} 15.5 ppm) and ¹¹B resonances (δ_{B} -41.6 ppm) similar to those of the precursor **2**. The coordination of a B-H bond to rhenium, however, is now indicated by the appearance in the ¹H NMR spectrum of a very broad resonance at -3.24 ppm corresponding to three H atoms, with a shielding higher than the one for free dppm·BH₃ (0.99 ppm),^{8b} but still lower than that of the hydride ligand of **3**, which appears at -10.60 ppm and displays similar couplings to two P atoms ($J_{\text{HP}} = 21, 16$), as found in **2**. It is then apparent that complex **3** undergoes in solution a dynamic exchange process between their B-H and B-H-Re hydrogens, fast on the NMR time scale. This is a common behavior for complexes displaying similar tricentric M-H-B interactions,²³ which was not further investigated for **3**. For comparison, the ¹H NMR resonance for the B-H-Re hydrogen in the mentioned *fac*-[Re{ $\kappa^2_{\text{s,s}}, \eta^2$ -H₂B(timMe)(bzt)}(CO)₃] complex (which does not undergo dynamic exchange with the terminal B-H hydrogen) appears at -6.62 ppm.²²

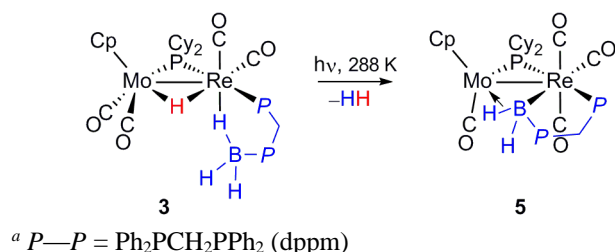
Structure of the Diphosphine-Bridged Complex 4. The IR spectrum of **4** also displays four C-O stretches, but with a pattern completely different from that of **3**, which now can be interpreted as arising from the presence in the molecule of a pyramidal or facial Re(CO)₃ fragment (three strong bands at 2001, 1912 and 1896 cm⁻¹),¹⁵ and a Mo(CO) fragment (one low-frequency band at 1793 cm⁻¹). This is consistent with the observation of just one ¹³C NMR resonance (δ_{C} 251.5 ppm) in the high-frequency region characteristic of Mo-bound carbonyls, and three resonances in the range 197.0-192.4 ppm corresponding to the Re-bound carbonyls. The ³¹P NMR spectrum of **4** displays three distinct resonances with normal widths, indicative of the absence of P-B connections in the molecule, also corroborated by the absence of BH₃ resonances in the corresponding ¹H and ¹¹B NMR spectra. The resonances for the inequivalent P atoms of the diphosphine ligand now appear at 76.3 and -14.6 ppm, with chemical shifts allowing their assignment to the Mo- and Re-bound P atoms of a bridging dppm ligand, respectively (cf. δ_{P} 64.3 ppm for [Mo₂Cp₂(μ -H)(μ -PCy₂)(CO)₂(μ -dppm)]).²⁵ The coordination sphere of the metal atoms is eventually completed with a cyclopentadienyl ligand at the Mo atom, and a hydride ligand bridging Mo and Re atoms (δ_{H} -11.55 ppm).

All of the above data define completely the stereochemistry around the Re atom. Besides this, we assume that the diphosphine ligand will be positioned as far away from

the Cp ligand as possible, to reduce steric repulsions. As a result, the only geometrical feature left to be defined for **4** is whether the Mo-bound P atom is positioned *cis* or *trans* relative to the PCy₂ group. A transoid positioning of these two P atoms would be favored on steric grounds, and is also indicated by the observation of a small P–Mo–P coupling of 7 Hz between these atoms.¹⁷ At the same time, such a positioning implies a *cis* arrangement of the Mo-bound PPh₂ group relative to the hydride ligand, hence a small P–Mo–H angle, then expectedly a large absolute value for the corresponding two-bond coupling,¹⁷ which indeed is consistent with the observation of a large P–H coupling of 44 Hz for the hydride resonance of **4**. In addition, the latter resonance displays smaller splittings of 19 and 9 Hz, corresponding to the couplings to the PCy₂ and Re–PPh₂ phosphorus atoms, they being comparable in magnitude to those observed for compounds **2** and **3**.

Photolysis of Compound 3. Although prepared at low temperature, the agostic complex **3** proved to be a thermally robust molecule, as no measurable change was observed upon refluxing a toluene solution of the complex for 1 h. In contrast, irradiation of toluene solutions of the complex with visible-UV light at 288 K for about 30 min caused its complete transformation, to give the diphosphine-boryl complex [MoReCp(μ - η^2 : κ^2 _{P,B}-H₂B·dppm)(μ -PCy₂)(CO)₄] (**5**) as major product (Scheme 3), which could be isolated in 60% yield after chromatographic workup.

Scheme 3. Dehydrogenation of the Agostic Complex 3^a



The formation of **5** from **3** requires the elimination of hydrogen involving the borane group and the hydride ligand, along with a significant spatial rearrangement of the *P*,*B*-donor ligand, coupled to the migration of a carbonyl ligand, from Mo to Re. It is then a rather complex and likely multistep reaction. The Gibbs free energy balance for the overall reaction (**3** → **5** + H₂) in the gas phase is +43 kJ/mol according to Density Functional Theory (DFT) calculations to be discussed below, which justifies our need to use photochemical procedures to induce this transformation (see the Experimental section for details). The close proximity of the hydride and the Re-bound H(B) atom in **3** (ca. 2.33 Å in the crystal; 2.28 Å according to DFT calculations) might facilitate a direct dehydrogenation process which, however, obviously is not possible under thermal conditions, but likely is triggered at one of the excited electronic states generated upon irradiation of **3**, a matter that might be worth of further study in the future. We should

note that, to our knowledge, the above reaction represents the first example of dehydrogenation in a coordinated dppm-BH₃ ligand. Such an *intramolecular* process can be related in some way to the *intermolecular* elimination of methane between the methyl complexes [MCp*(CO)₃Me] and BH₃·PMe₃ to give the corresponding boryl derivatives [MCp*(CO)₃(κ¹-BH₂·PMe₃)] (M = Mo, W), a process also induced photochemically.²⁶ In addition, it should be noted that there seems to be only one other complex previously characterized with the dppm-boryl ligand, the mononuclear cobalt complex [Co(κ²_{P,B}-H₂B·dppm)(CO)₂(κ¹-dppm)], a molecule prepared in low yield through direct reaction of CoCl₂ with Na(BH₄) in the presence of CO and dppm, and displaying a chelating coordination of the diphosphine-boryl ligand with no tricentric Co–H–B interactions.²⁷

Structure of Diphosphine-Boryl-Bridged Complex 5. The structure of **5** in the crystal (Figure 2 and Table 3) is made up of MoCp(CO) and T-shaped Re(CO)₃ fragments bridged by boryl and phosphanide ligands. The roughly octahedral coordination around rhenium is completed by the diphosphine-boryl ligand, with its “free” P atom coordinated *trans* to the PCy₂ group (P1–Re1–P2 = 178.9(1)^o). The boryl ligand can be viewed as bound to the rhenium atom through a conventional Re–B bond, and to the molybdenum atom through a tricentric Mo–H–B bond, both to be discussed in more detail below. In all, the diphosphine-boryl ligand then formally acts as a 5-electron donor in this novel μ-η²:κ²_{P,B} coordination mode, which in turn renders a count of 34 electrons for the complex. This is consistent with the intermetallic length of 3.075(1) Å in **5**, some 0.13 Å shorter than the corresponding distance in the precursor **3**, and much closer now to the reference value of 3.05 Å for a Mo–Re single bond.¹⁹ The phosphanide ligand is now placed some 0.08 Å closer to the Mo atom, likely to balance the relatively poor donor properties of the B–H group coordinated to this atom.

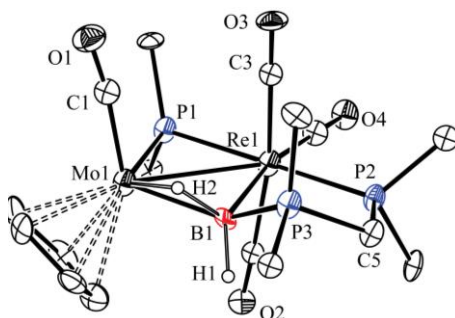


Figure 2. ORTEP diagram (30% probability) of compound **5** with Cy and Ph groups (except their C¹ atoms) and most H atoms omitted for clarity.

Table 3. Selected Bond Lengths (Å) and Angles (°) for Compound **5**

Mo1–Re1	3.075(1)	Mo1–P1–Re1	79.0(1)
Mo1–P1	2.379(4)	P1–Mo1–C1	86.4(5)
Re1–P1	2.455(3)	P1–Mo1–B1	101.5(4)
Re1–P2	2.398(3)	P1–Mo1–H2	121(4)
Mo1–B1	2.31(1)	C1–Mo1–H2	81(4)
Re1–B1	2.38(2)	P1–Re1–P2	178.9(1)
Mo1–C1	1.93(2)	P1–Re1–C2	88.8(4)
Mo1–H2	1.9(1)	P1–Re1–C3	86.7(4)
Re1–C2	2.00(2)	P1–Re1–C4	92.5(4)
Re1–C3	2.00(2)	P1–Re1–B1	97.4(4)
Re1–C4	1.90(2)	P2–Re1–C2	91.3(4)
B1–H2	1.2(1)	P2–Re1–C3	93.0(4)
B1–H1	1.12(5)	P2–Re1–C4	88.6(4)
P3–B1	1.92(2)	Mo1–H2–B1	94(4)
		C2–Re1–C3	169.1(6)

As noted above, the bridging boryl group in **5** can be viewed as σ -bound to Re and η^2 -bound to Mo, *via* one of the B–H bonds. In agreement with this, the Re–B distance is now quite short, 2.38(2) Å, close to the reference value of 2.35 Å for a Re–B single bond,¹⁹ and comparable to the corresponding values measured in the mononuclear complexes [Re(CO)₅(BCl₂)] (2.189(16) Å),²⁸ and [Re(CO)₅{B(NArCH)₂}] (2.292(4) Å),²⁹ which are the only other rhenium boryl complexes structurally characterized to date. As for the η^2 -coordination to Mo, we find now a quite reduced Mo–H–B angle of 94(4)°, and very short Mo–B separation of 2.31(1) Å, actually shorter than the reference value of 2.38 Å for a Mo–B single bond.¹⁹ These geometrical parameters therefore suggest that the tricentric Mo–H–B interaction in **5** should be clearly classified as one of the *side-on* type.²⁰ In this case, a search on the Cambridge Crystallographic Database revealed that this coordination mode typically involves Mo–B separations in the range 2.25–2.48 Å and Mo–H–B angles of 85–115°.³⁰ Thus, we can now speak of a rather tight *side-on* coordination to Mo of a B–H bond in compound **5**. As a further illustration of the above conclusion, we note that the Mo–B separation in **5** is ca. 0.2 Å shorter than the corresponding distances measured in the mononuclear phosphine-boryl complexes [MCp*(CO)₃(H₂B·PMe₃)] (M = Mo, W), which display conventional M–B bonds.²⁶

Spectroscopic data for compound **5** in solution (Table 1, Experimental Section, and SI) are consistent with the structure found in the solid state, and support its retention in solution. The IR spectrum of **5** displays four C–O stretches, which now can be interpreted as arising from the presence in the molecule of a meridional or T-shaped Re(CO)₃ fragment (bands at 2017, 1927 and 1905 cm⁻¹, with the most energetic one of weak intensity, as found in **2**),¹⁶ and a Mo(CO) fragment (one low-frequency band at 1761 cm⁻¹). This is in turn consistent with the observation of just one resonance in the high-frequency region of the ¹³C NMR spectrum (δ_c 245.4 ppm, Mo–CO), and three resonances in the range 195.7–188.9 ppm corresponding to the Re-bound carbonyls. The

Re-bound P atom of the diphosphine fragment displays a chemical shift slightly lower than the one measured for **3** (10.5 vs. 17.9 ppm) but its coupling to the bridging P atom is significantly reduced (55 vs. 100 Hz), perhaps due to the presence of more carbonyls around the Re atom in this molecule (cf. 70 Hz in **2**). Besides this, the Ph₂PBH₂ fragment gives rise to a ³¹P resonance comparable to that in **3** (23.7 vs. 15.5 ppm) whereas its ¹¹B resonance appears now much more deshielded (+14.2 vs. -41.6 ppm), in agreement with the closer approach of the B atom to the metal centers observed for **5**. This deshielding is in turn much higher than those measured for related terminal boryl complexes (cf. δ_{B} -24.6 to -31.7 ppm for [ML(CO)₃(κ^1 -H₂B·PMe₃)] complexes; M = Mo, W; L= Cp or Cp*),²⁶ in line with the respective M–B separations discussed above. Finally, we note that the ¹H NMR spectrum of **5** confirms the presence of two very different sites for the BH hydrogens, which give rise to quite broad resonances at ca. 5.65 and -11.87 ppm, sharpening significantly upon ¹¹B decoupling. These can be unambiguously assigned to the terminal B–H and bridging B–H–Mo hydrogens respectively, with the latter one displaying a nuclear shielding comparable to those of conventional bridging hydride ligands (cf. -11.5 to -13.1 ppm for compounds **2** to **4**). The latter can be taken as an additional spectroscopic indication that the tight *side-on* coordination of a B–H bond identified in the solid state is also retained in solution.

DFT Studies on the Agostic Complexes **3 and **5**.** As noted above, the photochemically-induced dehydrogenation of the coordinated diphosphine-borane ligand leading to the boryl complex **5** is a very unusual and likely a multistep process. Even if elucidation of the mechanism of this photochemical reaction falls outside the scope of the present work and exceeds our expertise, yet we have investigated the gas phase structures of compounds **3** and **5** and some on their potential isomers by using DFT methods (Figure 3 and Table 4; see the Experimental section for details),³¹ in search for some clues on likely dehydrogenation pathways. We were also interested in confronting the computed M–H–B interactions for **3** and **5**, found to be quite different from each other (*end-on* vs. *side-on*) both in solution and in the solid state, as discussed above.

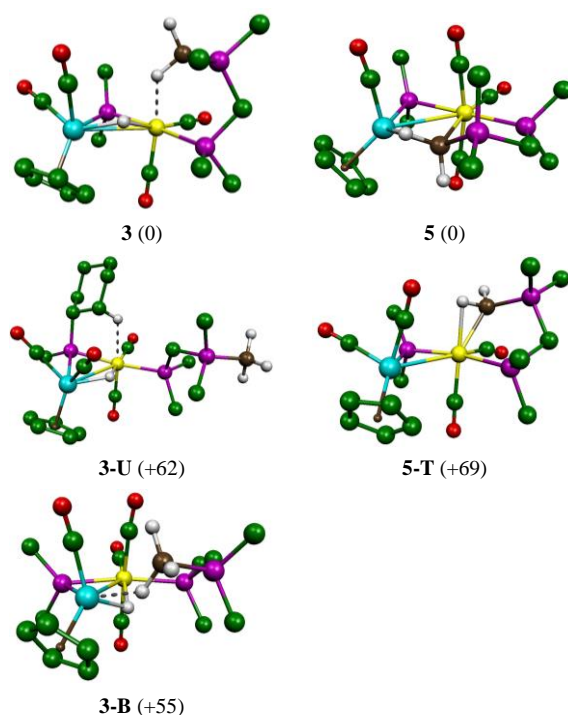


Figure 3. M06L-DFT-optimized structures of compounds **3** (left) and **5** (right), with Cy and Ph groups (except their C¹ atoms) and most H atoms omitted. Below them, some isomers for each are shown, with their relative Gibbs free energies at 298 K (in kJ/mol) indicated between brackets.

Table 4. M06L-DFT-computed Bond Lengths (Å) and Angles (°) for Compounds **3**, **5**, and some of their isomers.

parameter	3	3-B	5	5-T
Mo–Re	3.201	3.144	3.068	2.881
Mo–P1	2.506	2.455	2.387	2.469
Re–P1	2.395	2.435	2.482	2.380
Re–P2	2.391	2.395	2.399	2.425
Re–B	2.957		2.409	2.270
Mo–B		2.939	2.335	
M–HB	2.012	1.941	1.863	2.028
MH–B	1.240	1.235	1.298	1.243
BH	1.205/1.209	1.197/1.210	1.216	1.199
P1–Re–P2	169.1	161.3	179.7	165.4
M–H–B	129.2	134.3	93.5	84.2

First we note that the M06L-DFT optimized structures for **3** and **5** are in good general agreement with the corresponding structures determined in the solid state. In particular, the computed geometrical parameters for the Re–H–B interaction in **3** define a quite extreme *end-on* coordination of the B–H bond, as found in the crystal, with a very large Re···B separation of 2.957 Å and a Re–H–B angle of 129.2° (cf. 2.843(7) Å and 130(4)° in the crystal). The coordinated B–H bond (1.240 Å) is elongated by some 3% relative to the terminal B–H bonds (1.20 Å), which points to a relatively weak tricentric interaction in this case. In contrast, the computed parameters for the Mo–H–B interaction in **5** define a quite tight *side-on* coordination of the B–H bond, with a quite

short Mo–B separation of 2.335 Å and reduced Mo–H–B angle of 93.5° (cf. 2.31(1) Å and 94(4)° in the crystal). The coordinated B–H bond (1.298 Å) is now elongated by some 7% relative to the terminal B–H bond (1.216 Å), which indicates a much stronger interaction in this case.

Removing in compound **3** the relatively weak B–H coordination to Re leads to a genuine minimum structure (**3-U**) with a dangling Ph₂P·BH₃ group, while the rest of the molecule remains little perturbed (Figure 3, Mo–Re = 3.186 Å). The vacant coordination position left at the Re atom is now blocked by a Cy group, with one of the *ortho* hydrogens involved in a weak agostic C–H···Re interaction with the Re atom (H···Re = 2.283 Å). Isomer **3-U** is placed only 62 kJ/mol above **3**, but would have no obvious role in the dehydrogenation reaction of this complex.

We have also considered the possible formation of an isomer of **3** with the diphosphine-borane ligand bridging the Re and Mo atoms in a $\mu\text{-}\kappa^1:\eta^2$ mode (**3-B**), with an overall conformation similar to the one observed in the diphosphine-bridged complex **4**. Although this bridging coordination mode has not been yet reported for the dppm·BH₃ ligand, the computed parameters for the *end-on* Mo–H–B interaction in **3-B** are reasonable and comparable to those of the Re–H–B interaction in **3**, while the overall energy is only 55 kJ/mol higher, which makes it an affordable intermediate species. As concerning potential dehydrogenation processes, we note that the separation between hydride and Mo–H–B hydrogens in **3-B** is only 2.018 Å (cf. 2.279 Å in **3**).

Finally, we also examined alternative coordination modes for the diphosphine-boryl ligand present in the final product **5**, and found an energy minimum (**5-T**, 69 kJ/mol above **5**) with this ligand in a non-bridging chelating mode. Interestingly, the boryl-rhenium interaction in **5-T** also displays a tricentric Re–H–B interaction, with geometrical parameters now characteristic of *side-on* interactions (Re–B = 2.270 Å, Re–H–B = 84.2°, ReH–B = 1.243 Å),²¹ here imposed by the σ interaction of the boryl group with the same metal atom. We should finally note that, by recalling the analogy between L·BH₃ adducts and methane,^{23,26} the boryl coordination in structures **5** and **5-T** might be related to those of α -agostic bridging and terminal methyl complexes, respectively.^{20,32}

Concluding Remarks

Dppm·BH₃ readily displaces the acetonitrile ligand in the heterometallic hydride complex [MoReCp(μ -H)(μ -PCy₂)(CO)₅(NCMe)] under mild conditions, and expectedly coordinates the Re atom through its P atom, eventually yielding the pentacarbonyl complex [MoReCp(μ -H)(μ -PCy₂)(CO)₅(κ^1 _P-dppm·BH₃)], a thermally robust molecule displaying a transoid arrangement of the Re-bound P atoms, to minimize steric repulsions. The latter compound can be decarbonylated photochemically at low temperature, which triggers the coordination of a B–H bond of the dangling borane fragment to give the chelate complex [MoReCp(μ -H)(μ -PCy₂)(CO)₄(κ^1 _P, η^2 -dppm·BH₃)]. Extrusion of borane also takes place at a small extent during photolysis, this eventually yielding the diphosphine-bridged complex [MoReCp(μ -H)(μ -PCy₂)(CO)₄(μ -dppm)] as a side product. The chelate diphosphine-borane complex displays a tricentric Re–H–B interaction of *end-on* type, with the bridging hydrogen involved in fast exchange (on the NMR time scale) with the B–H hydrogens, which might anticipate hemilabile chemistry in solution. Extended photolysis of the latter complex at room temperature triggers an unprecedented, although endergonic, dehydrogenation involving the diphosphine-borane ligand and the bridging hydride, to give the diphosphine-boryl derivative [MoReCp(μ - η^2 : κ^2 _{P,B}-H₂B·dppm)(μ -PCy₂)(CO)₄], in a multistep process also involving migration of a carbonyl ligand, from Mo to Re. This complex displays a novel bridging coordination mode of the diphosphine-boryl ligand, with the boryl group being σ -bound to one metal (Re) and η^2 -bound to the other one (Mo) through a B–H bond. The corresponding tricentric Mo–H–B interaction is now of the *side-on* type and quite stronger, as revealed by the computed elongation of the B–H bond involved (7%, relative to the terminal B–H bond of the molecule), the strong magnetic shielding of the corresponding ¹H nucleus, and the absence of fast exchange with the uncoordinated H(B) atom.

Experimental Section

General Procedures and Starting Materials. All manipulations and reactions were carried out under an argon (99.995%) atmosphere using standard Schlenk techniques. Solvents were purified according to literature procedures, and distilled prior to use.³³ Compound **1**,⁴ and the adduct dppm·BH₃,^{8b, 34} (dppm = Ph₂PCH₂PPh₂) were prepared as described previously. Petroleum ether refers to that fraction distilling in the range 338–343 K. Photochemical experiments were performed using Pyrex Schlenk tubes cooled by tap water (ca. 288 K) or by a closed 2-propanol circuit kept at the desired temperature with a cryostat. A 400 W medium-pressure mercury lamp placed ca. 1 cm away from the Schlenk tube was used for these experiments. Filtrations were carried out

through diatomaceous earth unless otherwise stated. Chromatographic separations were carried out using jacketed columns cooled as described above. Commercial aluminum oxide (activity I, 70-290 mesh) was degassed under vacuum prior to use. The latter was mixed under argon with the appropriate amount of water to reach activity IV. IR stretching frequencies of CO ligands were measured in solution (using CaF₂ windows), are referred to as $\nu(\text{CO})$ and are given in wave numbers (cm⁻¹). Nuclear magnetic resonance (NMR) spectra were routinely recorded at 400.13 (¹H), 162.16 (³¹P{¹H}), 128.51 (¹¹B{¹H}), and 100.73 (¹³C{¹H}) MHz, at 298 K in CD₂Cl₂ solution unless otherwise stated. Chemical shifts (δ) are given in ppm, relative to internal tetramethylsilane (¹H, ¹³C), external BF₃·THF in THF (¹¹B) or external 85% aqueous H₃PO₄ solutions (³¹P). Coupling constants (J) are given in hertz.

Preparation of [MoReCp(μ -H)(μ -PCy₂)(CO)₅(κ^1 P-dppm·BH₃)] (2). Solid dppm·BH₃ (0.020 g, 0.050 mmol) was added to a solution of compound **1** (0.030 g, 0.041 mmol) in toluene (5 mL), and the mixture was refluxed for 10 min to give a yellow solution. The solvent was then removed under vacuum, the residue was extracted with dichloromethane/petroleum ether (1/2) and the extracts were chromatographed on an alumina column at 253 K. Elution with the same solvent mixture gave a yellow fraction yielding, after removal of solvents, compound **2** as a yellow solid (0.036 g, 81%). Anal. Calcd for C₄₇H₅₃BMoO₅P₃Re: C, 52.09; H, 4.93. Found: C, 51.75; H, 4.52. ¹H NMR: δ 7.99-6.98 (m, 20H, Ph), 4.79 (s, 5H, Cp), 3.92 (ddd, $J_{\text{HH}} = 15$, $J_{\text{HP}} = 12$, 7, 1H, PCH₂), 3.80 (ddd, $J_{\text{HH}} = 15$, $J_{\text{HP}} = 11$, 6, 1H, PCH₂), 2.61 (m, 1H, Cy), 2.39 (m, 1H, Cy), 2.07 (m, 1H, Cy), 2.01-0.97 (m, 19H, Cy), -13.09 (dd, $J_{\text{HP}} = 18$, 14, 1H, μ -H); the resonance of the BH₃ group could not be located precisely in this spectrum (Figure S3), it being partially obscured by the manifold Cy resonances. ¹¹B{¹H} NMR: δ -37.7 (br). ³¹P{¹H} NMR: δ 142.6 (d, $J_{\text{PP}} = 70$, μ -PCy₂), 13.3 (br, PB), -2.7 (dd, $J_{\text{PP}} = 70$, 11, ReP).

Preparation of [MoReCp(μ -H)(μ -PCy₂)(CO)₄(κ^1 P, η^2 -dppm·BH₃)] (3). A solution of compound **2** (0.030 g, 0.028 mmol) in toluene (5 mL) was irradiated with visible-UV light at 253 K for 5 min with a gentle N₂ (99.9995%) purge, to give a yellow solution. The solvent was then removed under vacuum, the residue was extracted with dichloromethane/petroleum ether (1/3) and the extracts were chromatographed on an alumina column at 288 K. Elution with the same solvent mixture gave a yellow fraction yielding, after removal of solvents, complex [MoReCp(μ -H)(μ -PCy₂)(CO)₄(μ -dppm)] (**4**) as a yellow solid (0.006 g, 20%). Elution with dichloromethane/petroleum ether (1/2) gave another yellow fraction, yielding analogously compound **3** as a yellow solid (0.020 g, 67%). The crystals used in the X-ray diffraction study of **3** were grown by the slow diffusion of a layer of petroleum ether into a concentrated dichloromethane solution of the complex at 253 K. *Data for compound 3:* Anal. Calcd for

C₄₆H₅₃BMoO₄P₃Re: C, 52.33; H, 5.06. Found: C, 52.51; H, 4.83. ¹H NMR: δ 7.60 (m, 2H, Ph), 7.52 (m, 2H, Ph), 7.49-7.27 (m, 14H, Ph), 7.22 (td, *J*_{HH} = 8, *J*_{HP} = 4, 2H, Ph), 4.72 (s, 5H, Cp), 3.96, 3.79 (2td, *J*_{HH} = 14, *J*_{HP} = 14, 9, 2 x 1H, PCH₂), 2.60, 2.50, 2.24 (3m, 3 x 1H, Cy), 2.11-1.00 (m, 19H, Cy), -3.24 (br, 3H, PBH₃), -10.60 (dd, *J*_{HP} = 21, 16, 1H, μ-H). ¹¹B{¹H} NMR: δ -41.6 (br). ³¹P{¹H} NMR: δ 153.1 (dd, *J*_{PP} = 100, 11, μ-PCy₂), 17.9 (AB dd, *J*_{PP} = 100, 81, Re-P), 15.5 (br, P-B). ¹³C{¹H} RMN (243 K): δ 245.0 (s, MoCO), 244.4 (d, *J*_{CP} = 23, MoCO), 201.4 (s, ReCO), 197.6 (s, ReCO), 141.2-120.9 (m, Ph), 90.2 (s, Cp), 52.6 [d, *J*_{CP} = 15, C¹(Cy)], 48.6 [d, *J*_{CP} = 13, C¹(Cy)], 36.9, 35.4 [2s, C²(Cy)], 35.0 [s, br, C²(Cy)], 34.0 [s, C²(Cy)], 29.1 [d, *J*_{CP} = 10, C³(Cy)], 28.75 [d, *J*_{CP} = 9, C³(Cy)], 28.7 [d, *J*_{CP} = 12, C³(Cy)], 28.5 [d, *J*_{CP} = 11, C³(Cy)], 27.0, 26.9 [2s, C⁴(Cy)], 25.3 (t, *J*_{CP} = 33, PCH₂). *Data for compound 4*. Anal. Calcd for C₄₆H₅₀MoO₄P₃Re: C, 53.02; H, 4.84. Found: C, 52.99; H, 4.81. ¹H NMR: δ 7.93 (m, 2H, Ph), 7.60-7.30 (m, 13H, Ph), 7.04 (m, 3H, Ph), 6.91 (m, 2H, Ph), 4.94 (s, 5H, Cp), 4.05 (dt, *J*_{HH} = 14, *J*_{HP} = 10, 1H, CH₂), 3.39 (ddd, *J*_{HH} = 14, *J*_{HP} = 12, 10, 1H, CH₂), 2.56 (m, 2H, Cy), 2.10-0.90 (m, 19H, Cy), -11.55 (ddd, *J*_{HP} = 44, 19, 9, 1H, μ-H). ³¹P{¹H} NMR: δ 122.1 (dd, *J*_{PP} = 19, 7, μ-PCy₂), 76.3 (dd, *J*_{PP} = 71, 7, MoP), -14.6 (dd, *J*_{PP} = 71, 19, ReP). ¹³C{¹H} RMN: δ 251.5 (m, MoCO), 197.0 (s, ReCO), 195.4 (dd, *J*_{CP} = 30, 10, ReCO), 192.4 (dd, *J*_{CP} = 56, 7, ReCO), 140.5 [d, *J*_{CP} = 43, C¹(Ph)], 139.9 [dd, *J*_{CP} = 40, 6, C¹(Ph)], 137.4 [dd, *J*_{CP} = 34, 5, C¹(Ph)], 136.2 [d, *J*_{CP} = 10, C²(Ph)], 135.8 [d, *J*_{CP} = 31, C¹(Ph)], 131.4-128.1 (m, Ph), 88.8 (s, Cp), 57.9 [d, *J*_{CP} = 10, C¹(Cy)], 48.6 [d, *J*_{CP} = 15, C¹(Cy)], 39.8, 36.4 [2d, *J*_{CP} = 5, C²(Cy)], 38.1 (dd, *J*_{CP} = 35, 30, PCH₂), 37.1, 36.9 [2d, *J*_{CP} = 3, C²(Cy)], 29.7, 29.3 [2d, *J*_{CP} = 9, C³(Cy)], 28.9, 28.5 [2d, *J*_{CP} = 11, C³(Cy)], 27.2, 27.1 [2s, C⁴(Cy)].

Preparation of [MoReCp(μ-η²:κ²_{P,B}-H₂B·dppm)(μ-PCy₂)(CO)₄] (5). A solution of compound **3** (0.030 g, 0.028 mmol) in toluene (5 mL) was irradiated with visible-UV light at 288 K for 30 min with a gentle N₂ (99.9995%) purge, to give an orange solution. The solvent was then removed under vacuum, the residue was extracted with dichloromethane/petroleum ether (1/1), and the extracts were chromatographed on an alumina column at 263 K. Elution with the same solvent mixture gave first a minor yellow fraction containing some uncharacterized species which was discarded, then an orange fraction yielding, after removal of solvents, compound **5** as an orange solid (0.018 g, 60%). The crystals used in the X-ray diffraction study of **5** were grown by the slow diffusion of a layer of petroleum ether into a concentrated toluene solution of the complex at 253 K. Anal. Calcd for C₅₃H₅₉BMoO₄P₃Re (**5**·C₇H₈): C, 55.55; H, 5.19. Found: C, 55.24; H, 4.85. ¹H NMR: δ 7.74, 7.66 (2m, 2 x 2H, Ph), 7.58-7.27 (m, 14H, Ph), 7.09 (m, 2H, Ph), 5.65 (vbr, 1H, BH), 5.06 (s, 5H, Cp), 4.41 (m, 2H, PCH₂), 2.50 (m, 1H, Cy), 2.37 (m, 2H, Cy), 2.14 (m, 1H, Cy), 2.04-0.98 (m, 18H, Cy), -11.86 (br, 1H, Mo-H-B). ¹H{¹¹B} NMR: δ 5.49 (s, 1H, BH), -11.87 (d, *J*_{PH} = 30, 1H, Mo-H-B)

$^{11}\text{B}\{^1\text{H}\}$ NMR: δ 14.2 (br). $^{31}\text{P}\{^1\text{H}\}$ NMR: δ 184.5 (dd, $J_{\text{PP}} = 55, 7$, $\mu\text{-PCy}_2$), 23.7 (br, PB), 10.5 (dd, $J_{\text{PP}} = 105, 55$, ReP). $^{31}\text{P}\{^1\text{H}\}$ NMR (213 K): δ 184.5 (d, br, J_{PP} ca 50, $\mu\text{-PCy}_2$), 25.3 (d, $J_{\text{PP}} = 105$, PB), 10.8 (dd, $J_{\text{PP}} = 105, 53$, ReP). $^{13}\text{C}\{^1\text{H}\}$ RMN (213 K): δ 245.4 (s, MoCO), 195.7, 192.4, 188.9 (3s, ReCO), 141.7-124.6 (m, Ph), 89.1 (s, Cp), 58.0, 48.8 [2s, br, $\text{C}^1(\text{Cy})$], 38.4, 35.9, 35.0, 34.2 [4s, $\text{C}^2(\text{Cy})$], 29.4 [s, br, $\text{C}^3(\text{Cy})$], 28.6-28.4 [m, br, $3\text{C}^3(\text{Cy})$ and PCH_2], 26.9, 26.6 [2s, $\text{C}^4(\text{Cy})$].

X-Ray Structure Determination of Compounds 3 and 5. Data collection for these compounds was performed at ca. 145 K on an Oxford Diffraction Xcalibur Nova single crystal diffractometer, using Cu $K\alpha$ radiation. Images were collected at a 62 mm fixed crystal-detector distance using the oscillation method, with 0.8 or 1.3° oscillation and variable exposure time per image. Data collection strategy was calculated with the program *CrysAlis Pro CCD*,³⁵ and data reduction and cell refinement was performed with the program *CrysAlis Pro RED*.³⁵ In the case of **3**, twinning was found to occur in the crystal. The experimental data were treated as two domain twinned data, the second domain being rotated from first one by 179.9993° around [1.00 0.00 0.00] (reciprocal axis) or [0.94 0.00 0.33] (direct axis). For both compounds, an empirical absorption correction was applied using the SCALE3 ABSPACK algorithm as implemented in the program *CrysAlis Pro RED*. Using the program suite WINGX,³⁶ the structures were solved by Patterson interpretation and phase expansion using SHELXL2016,³⁷ and refined with full-matrix least squares on F^2 using SHELXL2016. For compound **3**, all non-hydrogen atoms were refined anisotropically, and all hydrogen atoms were geometrically placed and refined using a riding model, except for H(1) to H(4), which were located in the Fourier maps and refined isotropically. Compound **5** crystallized with a disordered toluene molecule, satisfactorily modelled over two positions with half occupancies. In this case, all non-hydrogen atoms were refined anisotropically except for a few carbon atoms, which were refined isotropically to prevent their temperature factors from becoming non-positive definite. All hydrogen atoms were geometrically placed and refined using a riding model, except for H(1) and H(2), which were located in the Fourier maps and refined isotropically. Upon convergence, the strongest residual peaks (2.23-1.24 eÅ⁻³) were located around the metal atoms.

Computational Details. All DFT calculations were carried out using the GAUSSIAN09 package,³⁸ and the M06L functional.³⁹ A pruned numerical integration grid (99,590) was used for all the calculations *via* the keyword Int=Ultrafine. Effective core potentials and their associated double- ζ LANL2DZ basis set were used for Mo and Re atoms.⁴⁰ The light elements (P, B, O, C and H) were described with the 6-31G* basis.⁴¹ Geometry optimizations were performed under no symmetry restrictions, using initial coordinates derived from the X-ray data. Frequency analyses were performed for all the stationary points to ensure that a minimum structure with no imaginary

frequencies was achieved. Molecular diagrams and vibrational modes were visualized using the MOLEKEL program.⁴²

Supporting Information. A PDF file containing crystal data for compounds **3** and **5**, as well as IR and NMR spectra for new compounds, and a XYZ file including the Cartesian coordinates for all computed species. This material is available free of charge via the Internet at <http://pubs.acs.org>.

Author Information. Corresponding authors: E-mail: dgvivo@hotmail.com (D. G. V.), mara@uniovi.es (M. A. R).

Acknowledgment. We thank the MINECO of Spain and FEDER for financial support (Project CTQ2015-63726-P) and a grant (to E. H.), the SCBI of the Universidad de Málaga, Spain, for access to computing facilities, and the X-Ray unit of the Universidad de Oviedo for acquisition of diffraction data. D.G.-V. would like to thank the SEPE of Spain for unemployment support.

References

1. (a) Knorr, M.; Jourdain, I. Activation of alkynes by diphosphine- and μ -phosphido-spanned heterobimetallic complexes. *Coord. Chem. Rev.* **2017**, *350*, 217-247. (b) Mankad, N. P. Selectivity Effects in Bimetallic Catalysis. *Chem. Eur. J.* **2016**, *22*, 5822-5829. (c) Buchwalter, P.; Rosé, J.; Braunstein, P. Multimetallic Catalysis Based on Heterometallic Complexes and Clusters. *Chem. Rev.* **2015**, *115*, 28-126.
2. (a) Eisenhart, R. J.; Clouston, L. J.; Lu, C. C. Configuring Bonds between First-Row Transition Metals. *Acc. Chem. Res.* **2015**, *48*, 2885-2894. (b) Krogman, J. P.; Thomas, C. M. Metal-metal multiple bonding in C_3 -symmetric bimetallic complexes of the first row transition metals. *Chem. Commun.* **2014**, *50*, 5115-5127. (c) Thomas, C. M. Metal-Metal Multiple Bonds in Early/Late Heterobimetallic Complexes: Applications Toward Small Molecule Activation and Catalysis. *Comments Inorg. Chem.* **2011**, *32*, 14-38. (d) Ritleng, V.; Chetcuti, M. J. Hydrocarbyl Ligand Transformations on Heterobimetallic Complexes. *Chem. Rev.* **2007**, *107*, 797-858. (e) Collman, J. P.; Boulatov, R. Heterodinuclear Transition-Metal Complexes with Multiple Metal–Metal Bonds. *Angew. Chem. Int. Ed.* **2002**, *41*, 3948-3961.
3. (a) Oishi, M.; Oshima, M.; Suzuki, H. A Study on Zr–Ir Multiple Bonding Active for C–H Bond Cleavage. *Inorg. Chem.* **2014**, *53*, 6634-6654. (b) Oishi, M.; Kino, M.; Saso, M.; Oshima, M.; Suzuki, H. Early-Late Heterobimetallic Complexes with a Ta–Ir Multiple Bond: Bimetallic Oxidative Additions of C–H, N–H, and O–H Bonds. *Organometallics* **2012**, *31*, 4658-4661. (c) Kameo, H.; Nakajima, Y.; Suzuki, H. Drastic Acceleration of Phosphine/Phosphite Incorporation into a

- Tetrahydrido Ruthenium/Osmium Complex, and One-way Ruthenium to Osmium Migration of a Phosphorus Ligand. *Angew. Chem. Int. Ed.* **2008**, *47*, 10159-10162.
- (d) Clapham, S.; Braunstein, P.; Boag, N. M.; Welter, R.; Chetcuti, M. J. Carbon–Phosphorus Bond Cleavage in Allyldiphenylphosphine by a Heterobimetallic Ni=Mo Complex and Formation of an Electronically Unsaturated NiMo₂ μ -Diphenylphosphido Cluster. *Organometallics* **2008**, *27*, 1758-1764.
4. Alvarez, M. A.; García, M. E.; García-Vivó, D.; Huergo, E.; Ruiz, M. A. Acetonitrile Adduct [MoReCpCp(μ -H)(μ -PCy₂)(CO)₅(NCMe)]: A Surrogate of an Unsaturated Heterometallic Hydride Complex. *Inorg. Chem.* **2018**, *57*, 912-915.
 5. (a) Alvarez, M. A.; García, M. E.; García-Vivó, D.; Huergo, E.; Ruiz, M. A. Synthesis of the Unsaturated [MMoCp(μ -PR₂)(CO)₅][−] Anions (M = Mn, R = Ph; M = Re, R = Cy): Versatile Precursors of Heterometallic Complexes. *Eur. J. Inorg. Chem.* **2017**, 1280-1283. (b) Alvarez, M. A.; García, M. E.; García-Vivó, D.; Huergo, E.; Ruiz, M. A. Acceptor Behavior and E–H Bond Activation Processes of the Unsaturated Heterometallic Anion [MoReCpCp(μ -PR₂)(CO)₅][−] (Mo=Re). *Organometallics* **2018**, *37*, 3425-3436.
 6. Alvarez, M. A.; García-Vivó, D.; Huergo, E.; Ruiz, M. A. Trapping of an Heterometallic Unsaturated Hydride: Structure and Properties of the Ammonia Complex [MoMnCp(μ -H)(μ -PCy₂)(CO)₅(NH₃)].
 7. (a) Macías, R.; Rath, N. P.; Barton, L. [8,8- η^2 -{ η^2 -(BH₃)Ph₂PCH₂PPh₂}-*nido*-8,7-RhSB₉H₁₀]: A Rhodathiaborane with a Novel Bidentate Chelating Ligand. *Angew. Chem. Int. Ed.* **1999**, *38*, 162-164. (b) Volkov, O.; Macías, R.; Rath, N. P.; Barton, L. Phosphine-Boranes as Bidentate Ligands: Formation of [8,8- η^2 -{ η^2 -(BH₃)·dppm}-*nido*-8,7-RhSB₉H₁₀] and [9,9- η^2 -{ η^2 -(BH₃)·dppm}-*nido*-9,7,8-RhC₂B₈H₁₁] from [8,8-(η^2 -dppm)-8-(η^1 -dppm)-*nido*-8,7-RhSB₉H₁₀] and [9,9-(η^2 -dppm)-9-(η^1 -dppm)-*nido*-9,7,8-RhC₂B₈H₁₁], Respectively. *Inorg. Chem.* **2002**, *41*, 5837-5843.
 8. (a) Merle, N.; Frost, C. G.; Kociok-Köhn, G.; Willis, M. C.; Weller, A. S. Chelating Phosphane–Boranes as Hemilabile Ligands – Synthesis of [Mn(CO)₃(η^2 -H₃B·dppm)][BAr^F₄] and [Mn(CO)₄(η^1 -H₃B·dppm)][BAr^F₄]. *Eur. J. Inorg. Chem.* **2006**, 4068-4073. (b) Merle, N.; Kociok-Köhn, G.; Mahon, M. F.; Frost, C. G.; Ruggerio, G. D.; Weller, A. S.; Willis, M. C. Transition metal complexes of the chelating phosphine borane ligand Ph₂PCH₂Ph₂P·BH₃. *Dalton Trans.* **2004**, 3883-3892. (c) Ingleson, M.; Patmore, N. J.; Ruggerio, G. D.; Frost, C. G.; Mahon, M. F.; Willis, M. C.; Weller, A. S. Chelating Monoborane Phosphines: Rational and High-Yield Synthesis of [(COD)Rh{(η^2 -BH₃)Ph₂PCH₂PPh₂)][PF₆] (COD = 1,5-cyclooctadiene) *Organometallics* **2001**, *20*, 4434-4436.

9. Chaplin, A. B.; Scopelliti, R.; Dyson, P. J. The Synthesis and Characterisation of Bis(phosphane)-Linked (η^6 -*p*-Cymene)-ruthenium(II)-Borane Compounds. *Eur. J. Inorg. Chem.* **2005**, 4762-4774.
10. Yen, T. H.; Chu, K. T.; Chiu, W. W.; Chien, Y. C.; Lee, G. H.; Chiang, M. H. Synthesis and characterization of the diiron biomimics bearing phosphine borane for hydrogen formation. *Polyhedron* **2013**, *64*, 247-254.
11. Nguyen, D. H.; Bayardon, J.; Salomon-Bertrand, C.; Jugé, S.; Kalck, P.; Daran, J. C.; Urritigoity, M.; Gouygou, M. Modular Phosphole-Methano-Bridged-Phosphine(Borane) Ligands. Application to Rhodium-Catalyzed Reactions. *Organometallics* **2012**, *31*, 857-869.
12. For some recent reviews on this subject, see (a) Han, D.; Anke, F.; Trose, M.; Beweries, T. Recent advances in transition metal catalysed dehydropolymerisation of amine boranes and phosphine boranes. *Coord. Chem. Rev.* **2019**, *380*, 260-286. (b) Johnson, H. C.; Hooper, T. N.; Weller, A. S. The Catalytic Dehydrocoupling of Amine-Boranes and Phosphine-Boranes. In *Synthesis and Application of Organoboron Compounds. Topics in Organometallic Chemistry, vol 49*; Fernández, E., Whiting A. (Eds); Springer: Berlin, 2015, pp 153-220.
13. This intermediate species was identified by a strong C–O stretch in the IR spectrum at 2012 cm^{-1} , a hydride NMR resonance at -12.12 ppm ($J_{\text{HP}} = 22$, 13) and Rebound ^{31}P resonances at 125.3 ($\mu\text{-PCy}_2$) and -10.3 ppm (PPh_2), with mutual coupling of 25 Hz. These data compare well with the corresponding data for *fac*- $[\text{MoReCp}(\mu\text{-H})(\mu\text{-PCy}_2)(\text{CO})_5(\text{PPh}_2\text{H})]$: $\nu(\text{C-O})$ 2011 cm^{-1} ; δ_{H} -12.88 ($J_{\text{HP}} = 20$, 15); δ_{P} 126.8 ($\mu\text{-PCy}_2$) and -18.8 (PPh_2H), with $J_{\text{PP}} = 22$ Hz; see reference 4).
14. Inspection of the ^{31}P and ^1H NMR spectra of a crude reaction mixture revealed the presence of small amounts of the adduct $\text{dppm}\cdot\text{BH}_3$ and larger amounts of the double-adduct $\text{dppm}\cdot(\text{BH}_3)_2$ (for spectroscopic properties of the latter, see: Schmidbaur, H.; Stützer, A.; Bissinger, A.; Schier, A. Darstellung und Eigenschaften von Phosphanboranen polyfunktioneller Phosphanliganden; Kristallstrukturen des Bis(borantodiphenylphosphonio)methans und des Tetrakis[(borantodiphenylphosphonio)methyl]methans. *Z. Anorg. Allg. Chem.* **1993**, *619*, 1519-1525). So it seems that BH_3 is mainly lost as $\text{dppm}\cdot(\text{BH}_3)_2$. It is then plausible that formation of **4** is originated in a photochemical side reaction whereby **2** would partially decompose by losing $\text{dppm}\cdot\text{BH}_3$, which in turn would trap BH_3 from **2** to generate a boron-free intermediate.
15. Horton, A. D.; Mays, M. J.; Raithby, P. R. Synthesis and substitution reactions of a heterodimetallic molybdenum–manganese complex, $[\text{MoMn}(\mu\text{-H})(\mu\text{-PPh}_2)(\eta^5\text{-C}_5\text{H}_5)(\text{CO})_6]$; X-ray crystal structure of $[\text{MoMn}(\mu\text{-H})(\mu\text{-PPh}_2)(\eta^5\text{-C}_5\text{H}_5)(\text{CO})_4(\text{dppm}\text{-PP}')]$. *J. Chem. Soc., Dalton Trans.* **1987**, 1557-1563.

16. Braterman, P. S. *Metal Carbonyl Spectra*; Academic Press: London, U. K., 1975.
17. Two-bond coupling involving P atoms (${}^2J_{\text{PX}}$) in metal complexes increase algebraically with the P–M–X angle, and therefore are quite sensitive to the relative positioning of P and X. Their absolute values, however, do not follow the same trend in all cases, as the sign of coupling can change with angle. In octahedral environments, the absolute values for two-bond couplings usually follow the order $|{}^2J_{\text{cis}}| < |{}^2J_{\text{trans}}|$ but the reverse holds for piano-stool complexes of type MCpPXL₂. See, for instance, Jameson, C. J. In *Phosphorus-31 NMR Spectroscopy in Stereochemical Analysis*; Verkade, J. G., Quin, L. D., Eds.; VCH: Deerfield Beach, FL, 1987; Chapter 6, and Wrackmeyer, B.; Alt, H. G.; Maisel, H. E. Ein- und zwei-dimensionale Multikern NMR-Spektroskopie an den isomeren Halbsandwich-Komplexen *cis*- und *trans*- $[(\eta^5\text{-C}_5\text{H}_5)\text{W}(\text{CO})_2(\text{H})\text{PMe}_3]$. *J. Organomet. Chem.* **1990**, 399, 125-130.
18. Haupt, H. J.; Merla, A.; Flörke, U. Heterometallic Cluster Complexes of the Types $\text{Re}_2(\mu\text{-PR}_2)(\text{CO})_8(\text{HgY})$ and $\text{ReMo}(\mu\text{-PR}_2)(\eta^5\text{-C}_5\text{H}_5)(\text{CO})_6(\text{HgY})$ (R=Ph, Cy, Y=Cl, $\text{W}(\eta^5\text{-C}_5\text{H}_5)(\text{CO})_3$). *Z. Anorg. Allg. Chem.* **1994**, 620, 999-1005.
19. Cordero, B.; Gómez, V.; Platero-Prats, A. E.; Revés, M.; Echevarría, J.; Cremades, E.; Barragán, F.; Alvarez, S. Covalent Radii Revisited. *Dalton Trans.* **2008**, 2832-2838.
20. (a) Kubas, G. J. *Metal Dihydrogen and σ -Bond Complexes*; Kluwer Academic/Plenum: New York, USA, 2001. (b) Saillard, Y. J. in *Topics in Physical Organometallic Chemistry*; Gielen, M., Ed.; Freund Publishing House Ltd.: London, U.K., 1987; Vol. 2, Chapter 1.
21. Range of distances according to a search on the Cambridge Crystallographic Data Centre database (updated May 2019). The search yielded some 20 complexes having Re–H–BH connections, with roughly half of them displaying short Re–B distances in the range 2.28-2.46 Å and Re–H–B angles of 90-115° (*side-on* coordination), and half of them displaying large distances in the range 2.70-2.86 Å and Re–H–B angles in the range 115-150° (*end-on* coordination).
22. Videira, M.; Moura, C.; Datta, A.; Paulo, A.; Santos, I. C.; Santos, I. Rhenium(I) Tricarbonyl Complexes with Poly(azolyl)borates Generated in Situ from an Organometallic Precursor Containing the B–H \cdots Re Coordination Motif. *Inorg. Chem.* **2009**, 48, 4251-4257.
23. Shimoi, M.; Nagai, S.; Ichikawa, M.; Kawano, Y.; Katoh, K.; Uruichi, M.; Ogino, H. Coordination Compounds of Monoborane-Lewis Base Adducts: Syntheses and Structures of $[\text{M}(\text{CO})_5(\eta^1\text{-BH}_3\text{-L})]$ (M = Cr, Mo, W; L= NMe₃, PMe₃, PPh₃). *J. Am. Chem. Soc.* **1999**, 121, 11704-11712.

24. Garrou, P. Δ_R Ring Contributions to ^{31}P NMR Parameters of Transition-Metal-Phosphorus Chelate Complexes. *Chem. Rev.* **1981**, *81*, 229-266.
25. Alvarez, M. A.; García, M. E.; Ramos, A.; Ruiz, M. A. Reactivity of the Unsaturated Hydride $[\text{Mo}_2(\eta^5\text{-C}_5\text{H}_5)_2(\mu\text{-H})(\mu\text{-PCy}_2)(\text{CO})_2]$ toward P-donor Bidentate Ligands and Unsaturated N-Containing Organic Molecules. *Organometallics* **2007**, *26*, 1461-1472.
26. Kawano, Y.; Yasue, T.; Shimoi, M. BH Bond Activation of Trimethylphosphineborane by Transition Metal Complexes: Synthesis of Metal Complexes Bearing Nonsubstituted Boryl-Trimethylphosphine, $\text{Cp}^*\text{M}(\text{CO})_3(\text{BH}_2\cdot\text{PMe}_3)$ (M = Mo, W). *J. Am. Chem. Soc.* **1999**, *121*, 11744-11750.
27. Elliot, D. J.; Levy, C. J.; Puddephatt, R. J.; Holah, D. G.; Hughes, A. N.; Magnuson, V. R.; Moser, I. M. A Bridged Cobaltaborane Complex: First Structural Characterization of a Transition-Metal-BH₂ Bond. *Inorg. Chem.* **1990**, *29*, 5014-5015.
28. Bauer, J.; Braunschweig, H.; Dewhurst, R. D.; Kraft, K.; Radacki, K. Monohaloboryls (BHX⁻) as Bridging Ligands: Observable Dinuclear σ -(Halo)boranyl Intermediates in the Synthesis of Metalloborylenes. *Chem. Eur. J.* **2012**, *18*, 2327-2334.
29. Frank, R.; Howell, J.; Tirfoin, R.; Dange, D.; Jones, C.; Mingos, D. M. P.; Aldridge, S. Circumventing Redox Chemistry: Synthesis of Transition Metal Boryl Complexes from a Boryl Nucleophile by Decarbonylation. *J. Am. Chem. Soc.* **2014**, *136*, 15730-15741.
30. Range of distances according to a search on the Cambridge Crystallographic Data Centre database (updated May 2019). The search yielded some 75 complexes having Mo-H-BH connections, with most of them displaying short Mo-B distances in the range 2.25-2.48 Å and Mo-H-B angles of 85-115° (*side-on* coordination), and only about 1/4 of them displaying large distances in the range 2.70-2.98 Å and Re-H-B angles of 110-140° (*end-on* coordination).
31. (a) Cramer, C. J. *Essentials of Computational Chemistry, 2nd Ed.*; Wiley: Chichester, UK, 2004. (b) Koch, W.; Holthausen, M. C. *A Chemist's Guide to Density Functional Theory, 2nd Ed.*; Wiley-VCH: Weinheim, 2002.
32. (a) García, M. E.; Ramos, A.; Ruiz, M. A.; Lanfranchi, M.; Marchiò, L. Structure and Bonding in the Unsaturated Hydride- and Hydrocarbyl-Bridged Complexes $[\text{Mo}_2(\eta^5\text{-C}_5\text{H}_5)_2(\mu\text{-X})(\mu\text{-PCy}_2)(\text{CO})_2]$ (X= H, CH₃, CH₂Ph, Ph). Evidence for the presence of α -Agostic and π -Bonding Interactions. *Organometallics* **2007**, *26*, 6197-6212. (b) Alvarez, M. A.; García, M. E.; García-Vivó, D.; Ruiz, M. A.; Toyos, A. E-H Bond Activation and Insertion Processes in the Reactions of the

- Unsaturated Hydride $[W_2Cp_2(\mu-H)(\mu-PPh_2)(NO)_2]$. *Inorg. Chem.* **2018**, *57*, 2228-2241.
33. Armarego, W. L. F.; Chai, C. *Purification of Laboratory Chemicals, 7th ed.*; Butterworth-Heinemann: Oxford, U. K., 2012.
 34. Martin, D. R.; Merkel, C. M.; Ruiz, J. P. Borane and monoiodoborane derivatives of bis(diphenylphosphino)methane. *Inorg. Chim. Acta* **1986**, *115*, L29-L30.
 35. *CrysAlis Pro*; Oxford Diffraction Limited, Ltd.: Oxford, U. K., 2006.
 36. Farrugia, L. J. WinGX suite for small-molecule single-crystal crystallography. *J. Appl. Crystallogr.* **1999**, *32*, 837-838.
 37. (a) Sheldrick, G. M. A short history of SHELX. *Acta Crystallogr., Sect. A* **2008**, *64*, 112-122. (b) Sheldrick, G. M. Crystal structure refinement with SHELXL. *Acta Crystallogr., Sect. C* **2015**, *71*, 5-8.
 38. Frisch, M. J.; Trucks, G. W.; Schlegel, H. B.; Scuseria, G. E.; Robb, M. A.; Cheeseman, J. R.; Scalmani, G.; Barone, V.; Mennucci, B.; Petersson, G. A.; Nakatsuji, H.; Caricato, M.; Li, X.; Hratchian, H. P.; Izmaylov, A. F.; Bloino, J.; Zheng, G.; Sonnenberg, J. L.; Hada, M.; Ehara, M.; Toyota, K.; Fukuda, R.; Hasegawa, J.; Ishida, M.; Nakajima, T.; Honda, Y.; Kitao, O.; Nakai, H.; Vreven, T.; Montgomery, J. A., Jr.; Peralta, J. E.; Ogliaro, F.; Bearpark, M.; Heyd, J. J.; Brothers, E.; Kudin, K. N.; Staroverov, V. N.; Kobayashi, R.; Normand, J.; Raghavachari, K.; Rendell, A.; Burant, J. C.; Iyengar, S. S.; Tomasi, J.; Cossi, M.; Rega, N.; Millam, J. M.; Klene, M.; Knox, J. E.; Cross, J. B.; Bakken, V.; Adamo, C.; Jaramillo, J.; Gomperts, R.; Stratmann, R. E.; Yazyev, O.; Austin, A. J.; Cammi, R.; Pomelli, C.; Ochterski, J. W.; Martin, R. L.; Morokuma, K.; Zakrzewski, V. G.; Voth, G. A.; Salvador, P.; Dannenberg, J. J.; Dapprich, S.; Daniels, A. D.; Farkas, Ö.; Foresman, J. B.; Ortiz, J. V.; Cioslowski, J.; Fox, D. J.; *Gaussian 09, Revision A.02*; Gaussian, Inc.: Wallingford, CT, USA, 2009.
 39. Zhao Y.; Truhlar, D. G. A new local density functional for main-group thermochemistry, transition metal bonding, thermochemical kinetics, and noncovalent interactions. *J. Chem. Phys.* **2006**, *125*, 194101: 1-18.
 40. Hay, P. J.; Wadt, W. R. Ab initio effective core potentials for molecular calculations. Potentials for potassium to gold including the outermost core orbitals. *J. Chem. Phys.* **1985**, *82*, 299-310.
 41. (a) Hariharan, P. C.; Pople, J. A. Influence of polarization functions on MO hydrogenation energies. *Theor. Chim. Acta* **1973**, *28*, 213-222. (b) Petersson, G. A.; Al-Laham, M. A. A complete basis set model chemistry. II. Open-shell systems and the total energies of the first-row atoms. *J. Chem. Phys.* **1991**, *94*, 6081-6090. (c) Petersson, G. A.; Bennett, A.; Tensfeldt, T. G.; Al-Laham, M. A.; Shirley, W. A.; Mantzaris, J. A complete basis set model chemistry. I. The total energies of closed-

shell atoms and hydrides of the first-row elements. *J. Chem. Phys.* **1988**, *89*, 2193-2218.

42. Portmann, S.; Luthi, H. P. MOLEKEL: An Interactive Molecular Graphics Tool. *CHIMIA* **2000**, *54*, 766-770.

(For Table of Contents Use Only)

Table of Contents Synopsis

Coordination of $\text{Ph}_2\text{PCH}_2\text{PPh}_2 \cdot \text{BH}_3$ to the heterometallic hydride complex $[\text{MoReCp}(\mu\text{-H})(\mu\text{-PCy}_2)(\text{CO})_5(\text{NCMe})]$ eventually yielded an agostic derivative displaying *end-on* coordination of a B–H bond which, upon photolysis at room temperature, underwent dehydrogenation to render a diphosphine-boryl derivative displaying a novel bridging coordination mode, with a *side-on* coordination of a B–H bond.

Graphics for Table of Contents

